44th AIAA/ASME/SAE/ASEE Joint Propulsion Conference & Exhibit
21 - 23 July 2008, Hartford, CT

AIAA 2008-4502

# Swirl Effects on Shock Structure in Free Under-Expanded Supersonic-Nozzle Airflow

**A. Abdelhafez*** **and A. K. Gupta†**
Department of Mechanical Engineering, University of Maryland
College Park, MD 20742

**The effects of convective Mach number and air-fuel density ratio have been investigated experimentally under both non-swirling and swirling conditions in supersonic-nozzle flow comprising diamond shock structure with coaxial fuel injection. A convergent nozzle of inlet-to-exit area ratio of 25 was used to generate a free under-expanded supersonic airflow with maximum near-field Mach number of 2.0. Non-reacting conditions were considered, wherein fuel was simulated by helium and argon gases. Schlieren diagnostic technique with 6 ns exposure was implemented to allow for accurate visualization of shock structure by preventing any fluctuations of flowfield from showing up on the captured image. Two distinct diamond shock sub-structures were identified, namely a primary one generated off nozzle-rim and a secondary structure generated off the coaxial injection system and air-fuel shear layer. The primary shock sub-structure is affected mainly by the properties of airflow, whereas the secondary structure strongly depends on the properties of injected fuel, primarily convective Mach number. Imparting swirl to airflow results in significant reduction in the strengths of both primary and secondary structures, as compared to non-swirling conditions. Changing convective Mach number with swirl does not affect primary structure significantly; however, the secondary structure weakens with introduction of fuel injection and gradually diminishes with decrease in convective Mach number. No significant differences were observed with change in air-fuel density ratio.**



## I. Introduction

Hypersonic vehicles, powered by scramjet engines, are pivotal for the future of high-speed flight. The critical science issues in hypersonic research under in-flight conditions have not been fully understood yet. These issues include mixing and ignition in scramjet engines. Extensive investigation is still needed, in order to achieve better understanding of the complicated flow dynamics and chemistry involved with the final goal of improved efficiency and performance. Successful operation of any air-breathing system depends on efficient mixing, ignition, and combustion.[1] The efficiency and effectiveness of an injection system are defined by the achievable degree of fuel/air mixing and the system capability of minimizing injection-induced thrust losses, respectively.[2] Supersonic flows are compressible and resistant to fuel penetration and mixing. Therefore, the equivalence ratio of scramjet-engine operation has to be fuel-rich over a considerable part of the vehicle flight, in order to ensure that a flame is present to provide positive thrust. Any progress made on improving the engine efficiency must, therefore, be closely followed towards achieving efficient mixing between fuel and air. Scramjet flows have residence times of the order of only few milliseconds. In this short residence time, one must account for the mixing, ignition delay, and combustion time scales.

To shed some light on this technical challenge, Figure 1 shows a simplified chemical-kinetics analysis, similar to those conducted in previous research.[3,4] Plotted are the temporal variations of temperature for hydrogen/air mixtures of different equivalence ratios inside a plug-flow reactor. Fuel-rich conditions are considered, as is the case for actual scramjet operation. Perfect mixing is assumed, i.e., hydrogen mixes with air instantaneously and homogeneously over the entire reactor cross-section after injection. The inlet air temperature and Mach number are chosen to be 1000 K and 4.0, respectively, as common representatives of the conditions after the inlet and isolator sections of a hypersonic vehicle. The air temperature is assumed not to change with the injection of fuel. In an attempt to reduce ignition delay, adiabatic conditions are assumed here. This is unlike the analyses of previous research, i.e. the combustor walls are not cooled, as the actual operating conditions dictate. It can be seen from Figure 1 that the ignition delay increases from 0.25 to 1.0 ms with increase in equivalence ratio. Compared to the findings of previous research,[3,4] the assumption of adiabatic reactor helps in decreasing the ignition delay from 1.2 to 1.0 ms at high equivalence ratios, and the average value of ignition delay agrees well with the findings of other previous research, as well.[5,6] Nevertheless, the time scale of ignition delay is still considerably large, and if the assumption of perfect mixing is relieved, the mixing time scale and mixture non-homogeneity will have to be taken into consideration. Moreover, if wall cooling is incorporated, radical quenching must also be accounted for. In light of this analysis it can be seen how challenging the actual scramjet-engine operating conditions are, especially if

* Graduate Student, Student Member AIAA
† Distinguished University Professor, Fellow AIAA, E-mail: akgupta@umd.edu

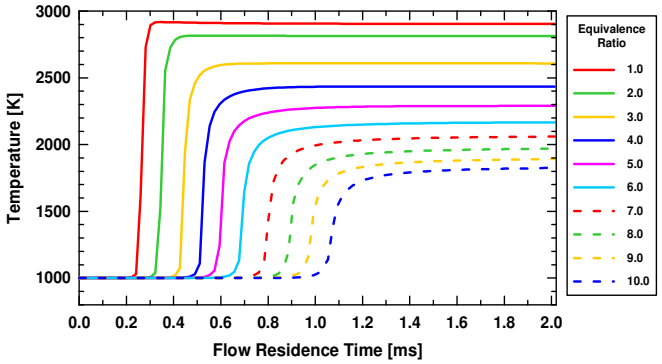


**Figure 1. Temporal temperature variation of an adiabatic, perfectly-stirred, plug-flow $H_2$/air reactor at different equivalence ratios of operation. Initial air Mach number and temperature = 4.0 and 1000 K, respectively.**

a target residence time of few milliseconds is to be met. Failure to meet such strict demands reflects on the engine length, which, in turn, affects the vehicle weight, available payload, developed thrust, and specific impulse.

Previous research has shown that flame holding in reacting supersonic flows is achieved by creating high-vorticity regions, where fuel and air partially mix at lower velocities.[7] In an experimental investigation,[8] a supersonic hydrogen flame, with coaxial injection, was stabilized successfully along the axis of a Mach-2.5 wind tunnel. Stabilization was achieved by using small-angled wedges mounted on the tunnel sidewalls to generate weak oblique shock waves that interact with the flame. It was found that these shock waves enhance fuel-air mixing to the extent that the flame length decreased by up to 30%, when certain shock locations and strengths were chosen that are optimum for the investigated geometry and operating conditions. The researchers reasoned that enhanced mixing resulted, in part, because the shocks induce radial inflows of air into the fuel jet. It was concluded that optimizing the mixing and stability limits for any combustor geometry requires careful matching of shock strengths and locations of shock/flame interaction.

In another investigation[9] shock-induced mixing was simulated numerically. Parallel flows of a heavy gas interspersed with other flows of a lighter one were overtaken by a normal shock wave. It was shown that vorticity is generated at each location of interaction of the density gradient across each light/heavy interface with the shock wave pressure gradient. Since the pressure and density gradient vectors are out of phase at these locations, their cross-product ($\nabla p \times \nabla \rho$) has non-zero values. This cross-product defines the Baroclinic vorticity vector, $\partial_t \vec{\omega}_{bc} = (\nabla p \times \nabla \rho)/\rho^2$, which causes the light gas regions to roll up into one or more counter-rotating vortex pairs, stirring and mixing the light and heavy gases together. It was concluded that, whenever possible, multiple shock waves should be utilized.

Shock waves of supersonic flows have significant positive effects on fuel-air mixing and flame stabilization, when they interact appropriately with the air/fuel shear layer. Some beneficial effects of this interaction[10] are: (a) directing the airflow locally towards fuel for increased entrainment rates, (b) creation of additional vorticity that enhances mixing, (c) elongation of the flame recirculation zones due to the adverse pressure gradient of a shock wave, and (d) increasing the flow static pressure and temperature through a shock wave. The exact role of each effect needs further substantiation and quantification.

Research on subsonic swirling flows is abundant in the literature; however, little of a fundamental nature is known about supersonic swirling ones. Imparting swirl to the fuel jet and/or supersonic airflow was shown to enhance mixing, especially in the near-field downstream of injection.[11-19] Therefore, to counter the adverse effects of compressibility, adding swirl is advantageous for mixing. Cutler et al.[11] experimentally investigated the effects of swirl and skew on the mixing of a supersonic light gas jet injected from a flat wall into a Mach-2.0 airstream. Their tests were conducted at nominally equal injectant mass flow rate and total pressure, as well as exit static pressure of injector nozzle. They concluded that the effect of combined swirl and skew on injectant mixing is to slightly increase mixing in the near-field of injection.

Yu et al.[12] performed an experimental study on mode-switching phenomena of supersonic jets with swirl. They observed that the shock-cell spacing of swirling jets is smaller than that of non-swirling ones, which suggests enhanced mixing. In non-swirling compressible jets, the typical two-dimensional vortex roll-up is believed to be suppressed, and mixing and entrainment are reduced, as compared to incompressible jets. Therefore, to counter the adverse effects of compressibility on mixing, adding swirl to a supersonic jet is favorable. The enhanced entrainment and mixing in swirling supersonic jets is thought to be due to the inherent three-dimensionality associated with the axial component of turbulent vorticity in swirling jets.

Kraus et al.[13] conducted an experimental study to determine whether the addition of swirl improves the mixing of a supersonic jet of fuel simulant (helium or air) injected at 30° to the wall into a confined Mach-2.0 airflow. Their results showed that the plumes from swirling and non-swirling jets had comparable penetration and area, but the swirling jets contained substantially less mass flow, which suggests better mixing efficiency. Carpenter[14] developed a linearized theory for under-expanded inviscid supersonic jets with arbitrary initial swirl. Estimates were made of the effect of swirl on the total radiated sound power of shock-associated noise. It was found that this noise can be greatly reduced, or even eliminated, at sufficiently high swirl levels, which can be achieved at the expense of a very small thrust loss. Noise elimination is believed to be due to enhanced mixing that leads to the disappearance of some initial shock cells.

Cutler et al.[15] proposed the addition of swirl to supersonic scramjet fuel jets as a method of enhancing fuel mixing. Enhanced mixing and flow recirculation were observed with the application of swirl, which was attributed to vortex breakdown. Yamasaki et al.[16] experimentally studied the effects of inlet swirl on the performance of a disk MHD generator. Their experiments were carried out using a novel disk MHD generator with 24 swirl vanes installed in a large shock-tube-driven facility. Remarkable improvements in both adiabatic and electrical efficiencies were observed by the introduction of inlet swirl. Dutton[17] investigated swirling flow in supersonic propulsion nozzles both numerically and experimentally. Computations were performed for a range of nozzle geometries, inlet swirl profiles, and swirl strengths. A time-dependent finite-difference technique was developed. The numerical results demonstrated, in agreement with the experimental data, that swirl has a minor effect on the specific impulse efficiency.

Kitamura et al.[18] conducted PIV measurements to investigate the effect of applying swirl to the supersonic fuel jets on air-fuel mixing in scramjet combustors. Their experimental data showed that application of swirl results in significant mixing enhancement. In a similar investigation, Yaguchi et al.[19] utilized PIV to study the effect of swirl on mixing in supersonic jets. Multiple swirl strengths were considered. Planar velocity distributions of single and twin supersonic jets were determined by PIV, with emphasis on maximum velocity decay and half-width spread. The researchers concluded that application of swirl promotes mixing.

The present work provides experimental investigation of the effect of imparting swirl to supersonic airflow. The effect of swirl on shock structure and mixing in supersonic flows has not been fully quantified in the literature yet, due to the intrinsic three-dimensional nature of the flow. Non-reacting conditions are considered, wherein helium and argon gases are used to simulate gaseous hydrogen fuel in under-expanded nozzle airflow containing diamond shock structure. The focus is to quantify the effects of convective Mach number and swirl on shock structure.

## II. Experimental Setup and Test Matrix

The experimental investigation of this present work has been performed on the UMD supersonic facility shown here in Figure 2. The utilized supersonic-nozzle assembly is shown schematically in Figure 3. A convergent nozzle of inlet-to-exit area ratio of 25 is used to generate a free under-expanded supersonic airflow. Reservoir pressures of up to about 9 atm (abs) are available, yielding near-field Mach numbers of up to 2.1. The nozzle has swirling capabilities, wherein the axial-tangential-entry technique with four tangential inlets is utilized to accurately control the degree of swirl imparted to airflow. This technique has been proven in previous research to be an efficient method for generating supersonic swirling jets.[15] A coaxial fuel-injection system injects helium (fuel-simulant) along the axis of air nozzle. The injection system can be positively and negatively recessed along the nozzle centerline to change the location of fuel injection with respect to airflow shock structure. A support flange upstream of nozzle ensures and maintains concentricity of the fuel injection system with respect to air nozzle, especially under swirling conditions. This flange, hatched blue in Figure 3, comprises a conical sleeve that embraces the injection system. The sleeve wall-thickness decreases in the direction of flow to provide streamlined performance and prevent any blockage close to the nozzle exit. The sleeve is held in place by three spokes extending to the support flange. The spokes are distributed evenly at 120° along tangential direction. Their thickness has been optimized to provide rigidity with minimum blockage to incoming axial component of airflow. It should be noted here that those spokes are located physically upstream of air tangential inlets and do not affect the flowfield of tangential air component. Some wakes are expected to exist in axial-component flowfield behind the spokes, but the supersonic flow exiting the nozzle was found to be fully axisymmetric in the presence as well as absence of tangential component.

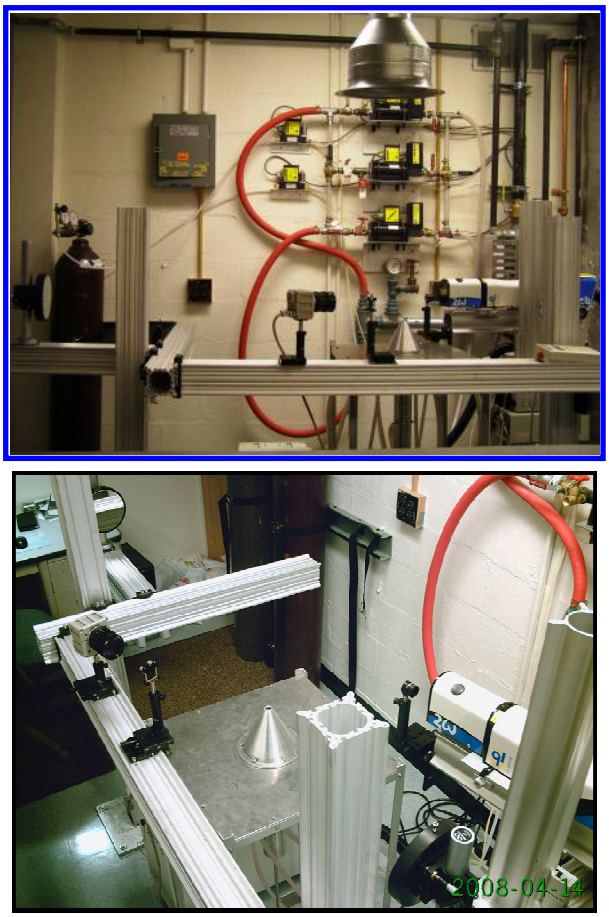


**Figure 2. Supersonic facility at UMD Combustion Laboratory**

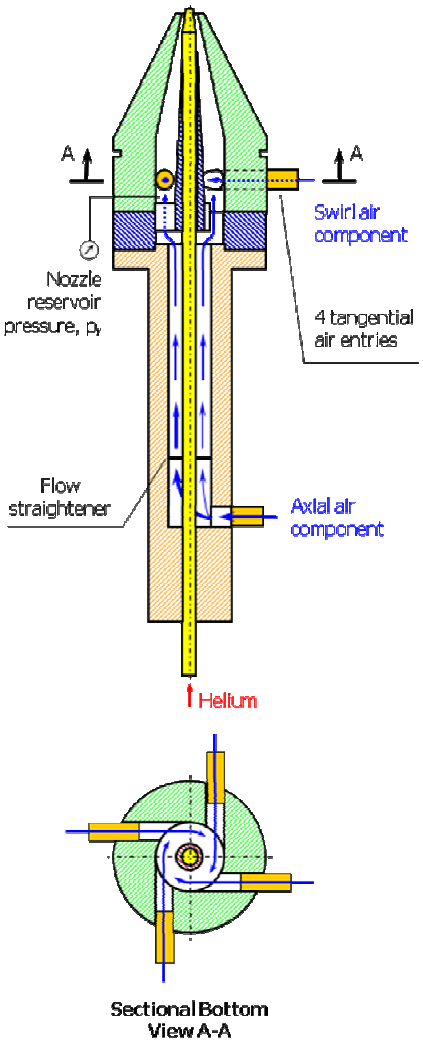


**Figure 3. Schematic of UMD supersonic-nozzle assembly**

The experimental results presented in this study have been obtained using nanosecond Schlieren diagnostic technique. A 532-nm Nd:YAG laser is used as the light source. The laser fires at 10 Hz with a pulse duration of only 6 ns. This short duration prevents any fluctuations of flowfield and shock structure from showing up on the captured image, thus allowing for accurate visualization of shock structure. Due to the collimated nature of the laser beam, a plano-concave lens increases the beam divergence, after the light intensity has been reduced to camera-safe levels through neutral-density filters. The divergent light beam fully illuminates a flow-scale concave mirror that reflects the light in a collimated fashion through the test section. After penetrating the flow, the light is focused by a concave mirror at a distant focal point. A knife-edge aperture intercepts the light path at the focal point to fulfill the Schlieren principles. A high-speed camera, synchronized with the laser, captures the resulting image at a resolution of 1024 x 1024 pixels. Figure 4 shows a schematic diagram of the nanosecond Schlieren system.

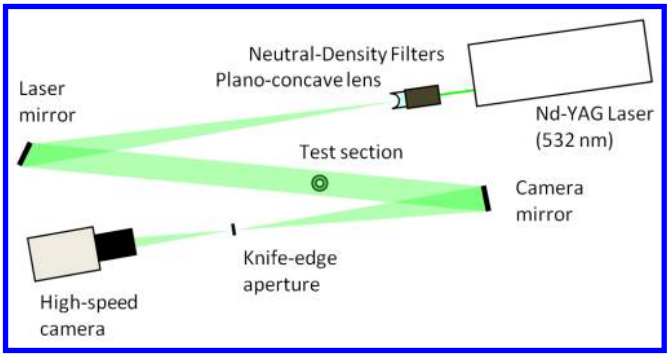


**Figure 4. Schematic of nanosecond Schlieren system**

Table 1 lists the test matrix for the results presented here. The effects of two flow parameters are investigated, namely convective Mach number and air-to-fuel density ratio. The former is defined here as:

$$M_{conv} = \frac{v_{air} - v_{fuel}}{a_{air}} = M_{air} - \frac{v_{fuel}}{a_{air}}$$

This definition relates the velocity difference between fuel and air to the speed of sound in air. It should be noted that the fuel stimulant is injected here at subsonic velocities, i.e., smaller than those of supersonic airflow. Therefore, the injectant velocity is subtracted from air velocity in our definition of convective Mach number, in contrast to the common definition given in literature.

Since the investigated under-expanded airflow undergoes an expansion fan after exiting the nozzle, the near-field Mach number is not constant. It increases from unity at the nozzle exit to a maximum value that prevails up to the first Mach disk. Nevertheless, the maximum value will be used in our definition of convective Mach number above. The shock structure and all properties of airflow, including the maximum near-field Mach number, depend on nozzle reservoir pressure and air total temperature. Both were kept constant at 7.8 atm (abs) and 300 K, respectively, for all the cases presented in this study. Based on isentropic ideal-gas relations, the corresponding maximum near-field Mach number of airflow equals 2.0. This value is concurred by the area-Mach-number relationship, which confirmed a Mach number of 2.0 at the maximum flow cross-sectional area downstream of the nozzle exit. Further details on the behavior of shock structure are given in the "Results and Discussion" section.

A total of 32 cases are presented here (16 non-swirling plus their 16 swirling counterparts). Due to the intrinsic three-dimensionality of swirling flows, no simple calculations of maximum near-field airflow Mach number could be done for the swirling cases. The non-swirling value of 2.0 was used instead. Nine case-pairs study the effect of convective Mach number, wherein the injectant (helium) velocity was changed. The remainder seven pairs study the effect of air-to-fuel density ratio with the injectant velocity kept fixed to

maintain a constant convective Mach number. The injectant, however, comprises different helium/argon mixtures, where mixture composition governs its density and, consequently, the overall air-to-fuel density ratio. Note that a letter "s" next to a case number in Table 1 denotes a swirling case.

Following a definition used for incompressible swirling jets,[20,21] a geometrical swirl number S is defined for air as

$$S_{air} = \left( \frac{\pi r_o R_o}{A_t} \right) \frac{m_t}{m_a + m_t}$$

where, $(\pi r_o R_o / A_t)$ = 0.68, for the geometry of the used nozzle and its tangential entries. ($m_a$) and ($m_t$) are the axial and tangential components of airflow, respectively. These flow rates were controlled and measured using thermal flow controllers of ±1.5% full-scale accuracy.

**Table 1. Test Matrix**

Nozzle reservoir pressure = 8 atm, abs. (constant)
Air total temperature at inlet = 300 K (constant)
Maximum near-field air Mach number = 2.0 (constant)
Swirl number for swirling cases, $S_{air}$ = 0.68 (constant)

| Case | Injected Gas | Convective Mach Number | Density Ratio |
|---|---|---|---|
| Effect of Convective Mach Number | | | |
| 1 & 1s | Helium | 1.91 | 36.73 |
| 2 & 2s | | 1.86 | |
| 3 & 3s | | 1.81 | |
| 4 & 4s | | 1.77 | |
| 5 & 5s | | 1.72 | |
| 6 & 6s | | 1.67 | |
| 7 & 7s | | 1.63 | |
| 8 & 8s | | 1.58 | |
| 9 & 9s | | 1.53 | |
| Effect of Density Ratio | | | |
| 10 & 10s | Helium/Argon mixture | 1.42 | 4.48 |
| 11 & 11s | | | 5.03 |
| 12 & 12s | | | 5.74 |
| 13 & 13s | | | 6.68 |
| 14 & 14s | | | 7.98 |
| 15 & 15s | | | 9.93 |
| 16 & 16s | | | 13.12 |

A constant air swirl number of 0.68 was maintained for all swirling cases. No simple calculations could be done to account for the flow compressibility or any change in swirl number, as the flow switches from elliptic subsonic to hyperbolic supersonic propagation at nozzle exit. It should be noted that none of the existing definitions of swirl number is ideal, as they represent integral effects only and not the detailed jet exit-velocity profiles that should be taken into consideration.[22,23]

## III. Results and Discussion

**Shock Structure (Non-Swirling, No Fuel Injection)**

The diamond shock structure of simple free under-expanded supersonic flow is shown schematically in Figure 5a. Also shown, for comparison, is shock structure of over-expanded flow in Figure 5b. As can be seen, both structures comprise the same shock-cell unit that gets repeated periodically to form the diamond shock-cell train. This unit is highlighted with dashed green boundaries in Figure 5 and can be described as follows. Axial under-expanded flow undergoes an expansion fan and turns outwards. The free-jet boundary adapts accordingly and turns outwards as well. Passing again through the expansion fan, the maximum near-field Mach number is reached, and the outward flow turns back to axial. As the expansion fan meets the boundary, it reflects into a compression fan that coalesces later into a shock wave. The annular flow adjacent to boundary turns inwards through the compression fan, and the boundary again adapts by turning inwards as well. The compression-fan shock terminates into a normal Mach disk, from which another shock wave originates to turn the inward annular flow back to the axial direction. Since the Mach disk maintains the axial direction of core flow, the entire flow is now axial again. As the originated shock wave impinges on flow boundary, it reflects into an expansion fan, starting another shock-cell unit.

Since coaxial injection has been implemented in all cases to be presented here, more emphasis will be placed on the core of airflow as well as the changes it undergoes. As seen from Figure 5a, most of the distance travelled by core flow from nozzle exit to first Mach disk is after expansion, i.e., at maximum near-field Mach number. This further explains the choice of maximum Mach number in calculation of convective Mach number, as indicated earlier.

In presence of a coaxial injection system, the shock structure differs significantly from the simple one described above. Figure 6 shows a Schlieren image as well as a schematic of the shock structure of free nozzle flow in the presence of a non-recessed coaxial injection system with no fuel injection. Two distinct sub-structures are identifiable from Schlieren image and highlighted in separate colors in the schematic. The sub-structure marked black is the simple nozzle-rim structure discussed above. A new sub-structure, marked here in red, is generated due to the existence of coaxial injection

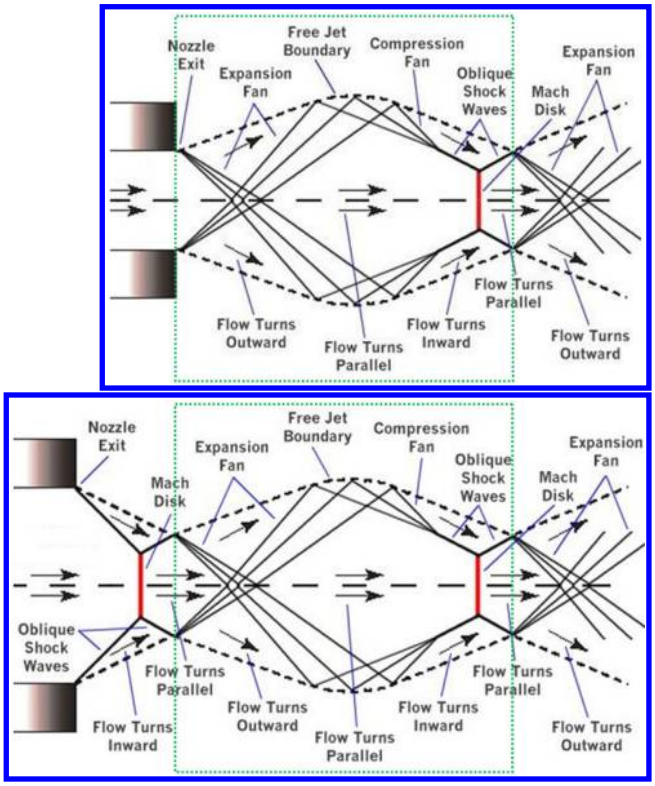


**Figure 5. Schematic of diamond shock structure of simple free nozzle flow, (a) under-expanded and (b) over-expanded**

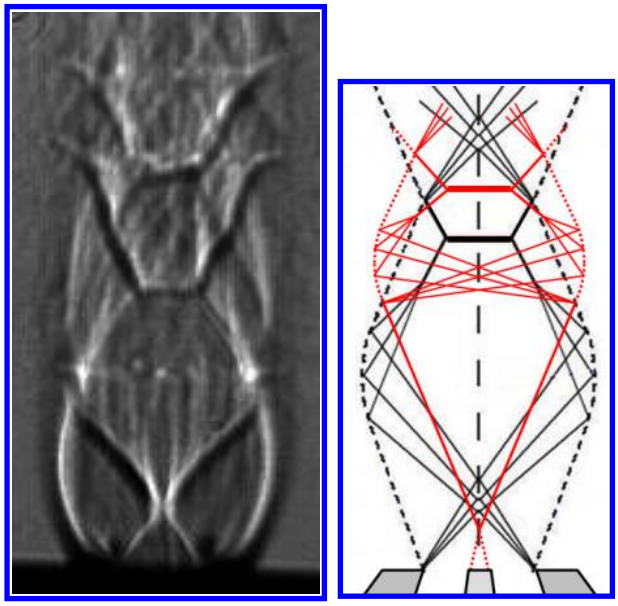

**Figure 6. Shock structure of free under-expanded nozzle flow in presence of non-recessed coaxial injection system with no fuel injection**

system. It should be noted here that both sub-structures are not fully independent of each other. The presence of each affects the other. This interaction is, however, not indicated on the schematic in Figure 6, for easier understanding of the newly introduced sub-structure from the injection system. Indicated here is how each structure would propagate if fully independent of the other. From this point forward, the nozzle-rim and injection-system sub-structures will be denoted "primary" and "secondary" shock structures, respectively, in this study.

The secondary structure starts with the airflow generating an inner conical boundary that completes the cone-frustum shape of fuel system tip. At the centerline, the flow collapses into itself, generating a conical shock wave that turns the flow back to parallel. This shock wave impinges on the outer flow boundaries shortly downstream of the impingement location of nozzle-rim expansion fan. The outer boundaries are altered by the impingement of that conical shock as observed from Figure 6. The shock reflects into an expansion fan that creates its own compression fan, shock waves, and Mach disk, similar to the primary structure generated by nozzle-rim expansion fan. Both Mach disks of primary and secondary structures appear distinctly.

The effect of coaxial fuel injection is shown in Figure 7. Helium is used as fuel stimulant. As observed, the secondary shock structure is altered slightly. A shear layer develops in place of the former inner conical boundaries of airflow. Due to the presence of helium, the shear layer does not converge to a sharp point at the centerline. Moreover, due to the curved shape of this shear layer, the airflow undergoes a compression fan first that collapses later into a shock wave.

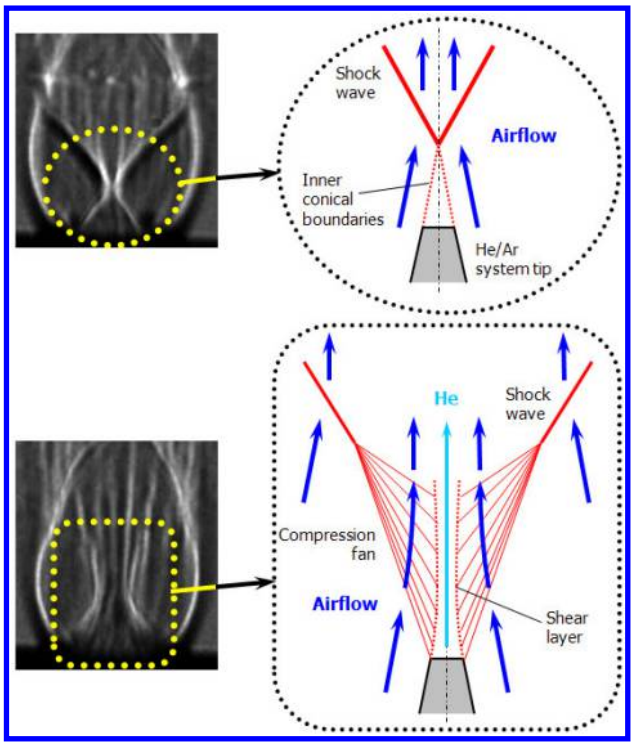


**Figure 7. Effect of fuel injection on shock structure of free under-expanded nozzle flow in presence of non-recessed coaxial injection system**

### Effect of Convective Mach Number (Non-Swirling)

The effect of air-helium convective Mach number is examined under non-swirling conditions in cases 1 – 9 given in Table 1. Keeping all air properties constant, the flow rate of helium was changed to induce different helium velocities and thus various convective Mach numbers, based on the aforementioned discussion. The Mach number of helium was maintained below 0.3 to avoid any compressibility effects on the helium-side of air/helium shear layer and to maintain a constant helium density. This resulted in a fixed air-to-helium density ratio of 36.73 for all the nine cases.

As helium injection is introduced, the flow structure transitions from the schematic shown on the left in Figure 8 to the one shown in the middle, as was also described earlier in Figure 7. If convective Mach number is decreased (i.e., helium velocity increased), the compression fan collapses earlier. This trend is expected to prevail, until the compression fan is almost replaced by a single shock wave originating from the fuel-system tip, as shown to the right in Figure 8. The early collapse moves the shock physically upstream, together with its location of impingement on the outer flow boundaries. The further upstream this location becomes, the more the primary and secondary Mach disks approach each other, as observed from Figure 9. This finding is further strengthened by Figure 10, which shows the variations in axial locations of first primary and secondary Mach disks with convective Mach number. The locations are referenced to the nozzle-exit plane and normalized by the nozzle-exit diameter (11 mm). Digital image processing of Schlieren images (Figure 9) was performed in Matlab to determine the locations of Mach disks by tracking the positions along flow centerline where the intensity sharply drops, since the disks are distinctly identifiable by their relatively darker shade. It can be observed from Figure 10 that both Mach disks approach each other, as the convective Mach number is decreased. It should be noted, however, that the secondary shock sub-structure is more susceptible to changes in convective Mach number than the primary structure. While the axial location of first secondary Mach disk decreases by a total of 18% from cases 1 to 9, the location of first primary disk increases by 7% only. This behavior is expected, as the secondary structure is generated off the injection system and air-helium shear layer. Nevertheless, the effect of changing convective Mach number across shear layer is not limited to secondary structure alone. Both structures are affected (to different extents), since they are intrinsically dependent, as discussed earlier. It is worth recalling here that the airflow properties were maintained constant, whereas those of helium were varied to induce changes in convective Mach number.

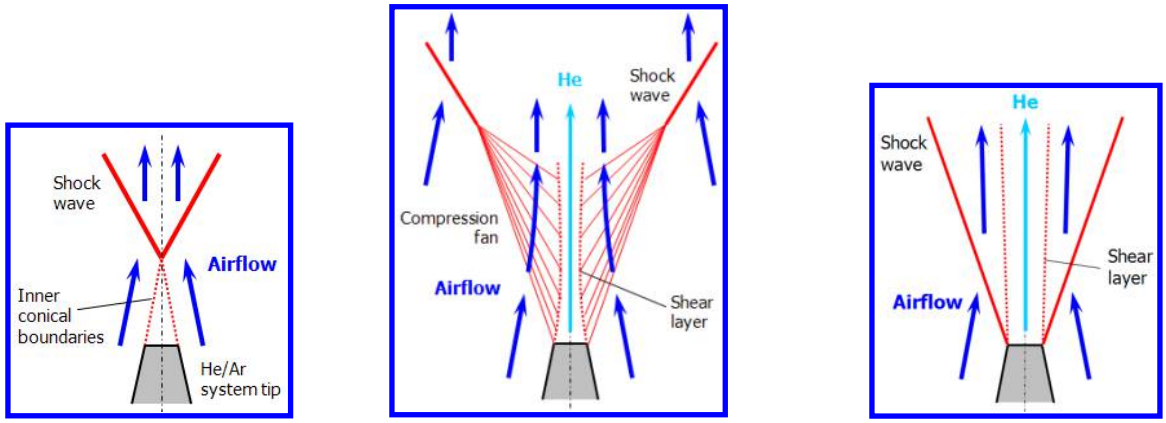


**Figure 8. Schematic comparison of flow structure at high (left), medium (middle), and low (right) convective Mach number**

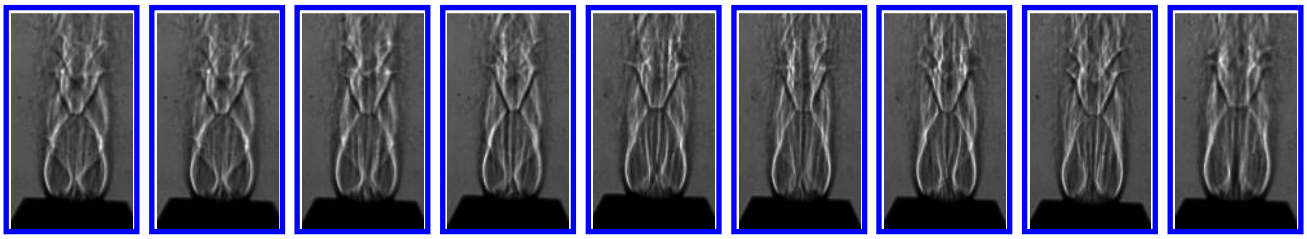

| Case # | 1 | 2 | 3 | 4 | 5 | 6 | 7 | 8 | 9 |
|---|---|---|---|---|---|---|---|---|---|
| $M_{conv}$ = | 1.91 | 1.86 | 1.81 | 1.77 | 1.72 | 1.67 | 1.63 | 1.58 | 1.53 |

**Figure 9. Effect of convective Mach number under non-swirling no-recess conditions (constant density ratio = 36.73)**

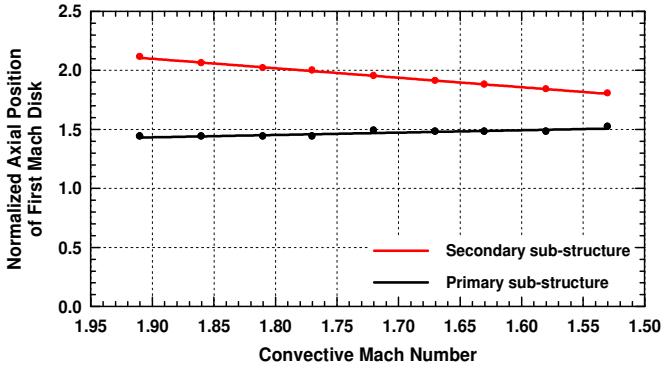


**Figure 10. Effect of convective Mach number on axial position of primary and secondary first Mach disks; position is normalized by nozzle-exit diameter (11 mm)**

### Effect of Density Ratio (Non-Swirling)

The effect of air-fuel density ratio is examined also under non-swirling conditions in cases 10 – 16 given in Table 1. All air properties have been again kept constant at the values listed in Table 1. Different mixtures of helium and argon gases were injected coaxially to simulate fuel. The mixture composition was changed from one case to the other to induce different mixture densities and thus various air-fuel density ratios. The flow rate of He-Ar mixture was adjusted to adapt for its changing density and maintain a constant velocity, which resulted in a constant air-fuel convective Mach number of 1.42.

Figure 11 provides a side-by-side comparison of the Schlieren images of cases 10 to 16. Unlike what was observed in the analysis of convective Mach number, changing the air-fuel density ratio does not induce significant changes in either shock sub-structures. This statement is concurred by Figure 12, which shows the effect of air-fuel density ratio on variation of axial positions of first primary and secondary Mach disks. No significant increases or decreases are observed in either position, and both Mach disks do not approach each other, as was the case earlier in the analysis of convective Mach number.

Combining the findings of both convective Mach number and density ratio analyses, the following key conclusions can be made: (a) The primary shock sub-structure is affected mainly by properties of airflow. Keeping these unchanged results in an almost constant primary structure that undergoes only minor changes due to its partial dependence on secondary structure. (b) The secondary structure, generated off injection system and air-fuel shear layer, is strongly dependent on properties of injected fuel, primarily convective Mach number. (c) Changing convective Mach number alters the ability of central fuel jet to influence curvature of shear layer and, consequently, the secondary sub-structure it generates. (d) The effect of changing air-fuel density ratio at constant convective Mach number does not propagate across the compressible supersonic-to-subsonic air-fuel shear layer, which does not undergo significant changes in shape and curvature. Therefore, the secondary structure remains unaffected.

### Introduction of Swirl to Airflow (No Fuel Injection)

Up to this point, only non-swirling conditions have been considered. The introduction of swirl to supersonic airflow results in substantial changes in entire flowfield, affecting both primary and secondary shock sub-structures. Figure 13 compares the Schlieren images of non-swirling and swirling flowfields in the absence of fuel injection. Further image processing in Matlab was performed on the image to the right (swirling) to illuminate the background, thus increasing the contrast between shock structure and background for easier visualization of the former.

Based on the comparison of Figure 13, imparting swirl to airflow results in the following observations: (a) The strengths of both primary and secondary sub-structures are reduced significantly, considering the shock thickness as an indicator of shock strength. (b) A considerably larger dark region is identifiable immediately downstream of nozzle exit. This region comprises a larger nozzle-rim expansion fan and a newly formed minor compression fan. Such compression fan does not exist in the non-swirling flowfield, as the flow forms conical inner boundaries that terminate at

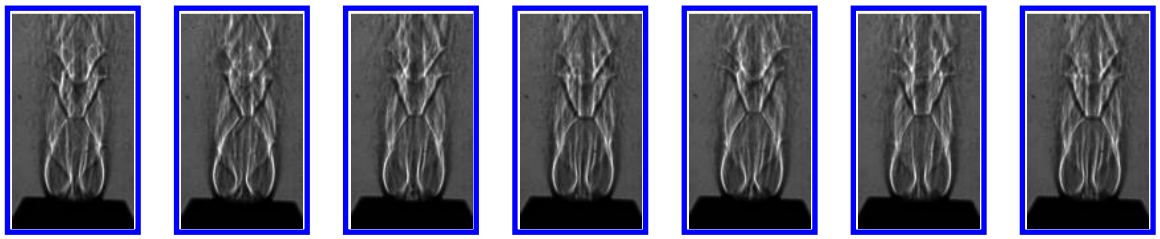

| Case # | 10 | 11 | 12 | 13 | 14 | 15 | 16 |
|---|---|---|---|---|---|---|---|
| DR = | 4.48 | 5.03 | 5.74 | 6.68 | 7.98 | 9.93 | 13.12 |

**Figure 11. Effect of density ratio (DR) under non-swirling no-recess conditions (constant convective Mach number = 1.42)**

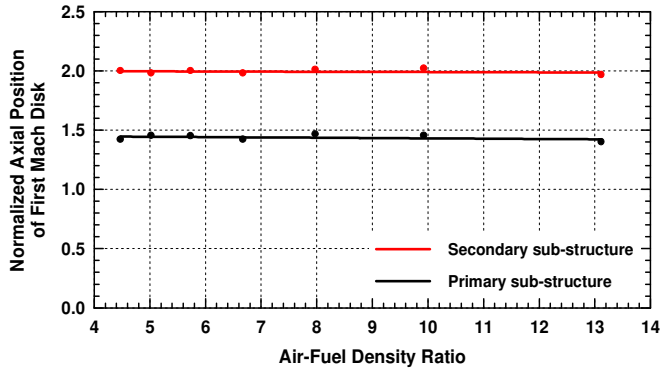


**Figure 12. Effect of air-fuel density ratio on axial position of primary and secondary first Mach disks; position is normalized by nozzle-exit diameter (11 mm)**

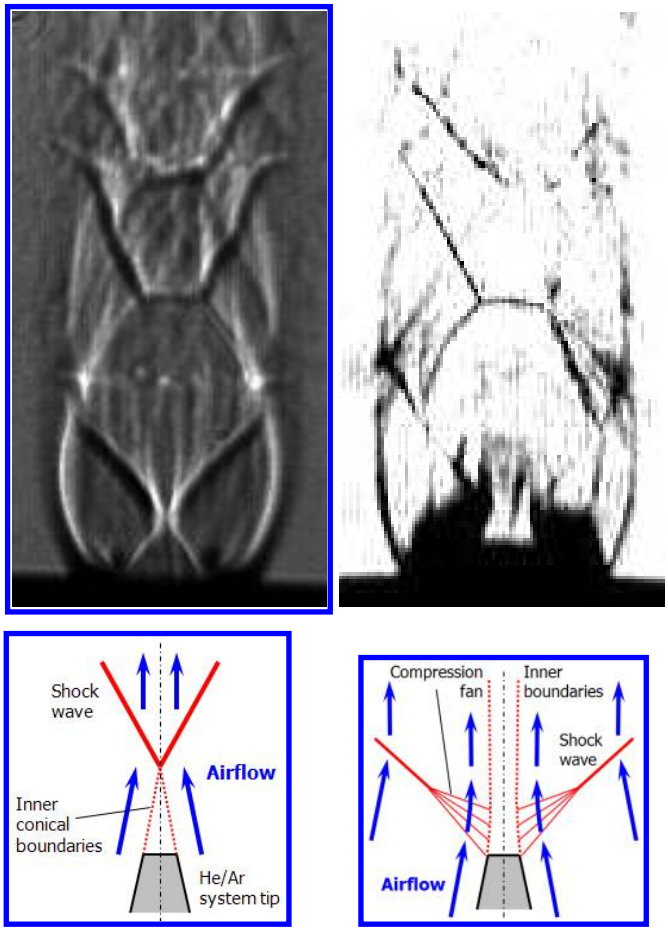


**Figure 13. Shock structures of non-swirling (left) and swirling (right) free under-expanded nozzle flow in presence of non-recessed coaxial injection system with no fuel injection**

the centerline into a sharp conical shock wave. However, in the swirling flowfield the centrifugal force pushes airflow outwards, resulting in the formation of inner flow boundaries that do not terminate at the centerline. The new minor compression fan is formed as airflow turns gradually to parallel along those inner boundaries. Similar to all other compression fans in the flow, the newly formed one coalesces into a shock wave that propagates to the flow outer boundaries, reflects, and forms the secondary sub-structure.

### Effect of Convective Mach Number (Swirling)

The effect of air-helium convective Mach number is examined under swirling conditions in cases 1s – 9s given in Table 1. Maintaining the same nozzle reservoir pressure and air total temperature of the non-swirling cases, entire airflow was fed through nozzle tangential inlets to induce a swirl number of 0.68, based on aforementioned definition. Assuming that the value of maximum near-field Mach number of airflow holds at 2.0 under swirling conditions, the same helium-flow properties in non-swirling cases 1 – 9 were repeated for the swirling ones 1s – 9s. This allowed for investigation of the same nine values of convective Mach number under swirling conditions.

Figure 14 provides a side-by-side comparison of the Schlieren images of cases 1s – 9s. It can be observed that changing convective Mach number does not have any significant effects on primary shock sub-structure. This is expected, since primary structure depends mainly on airflow properties, based on abovementioned discussion. The secondary structure, on the other hand, weakens with introduction of helium injection and gradually diminishes with decrease in convective Mach number. As helium velocity is increased, the shape of air-helium shear layer is altered. The smallest alterations are sufficient to induce significant changes in the newly formed compression fan, the shock wave it coalesces into, and thus the entire secondary sub-structure. If this new compression fan gets swallowed into the larger nozzle-rim expansion fan of swirling flowfield, the origin of secondary structure is eliminated, and the swirling flowfield comprises primary structure solely. Such behavior was not encountered in non-swirling flowfield, since its nozzle-rim expansion fan is of smaller size, which does not allow for much interference with the compression fan that generates off air-helium shear layer and forms secondary shock sub-structure.

### Effect of Density Ratio (Swirling)

Cases 10s – 16s of Table 1 highlight the effect of air-fuel density ratio under swirling conditions. The same He-Ar mixtures injected in non-swirling cases 10 – 16 were again injected in swirling ones (cases 10s – 16s) to allow for investigation of the same seven values of air-fuel density ratio under swirling conditions. Figure 15 shows a side-by-side comparison of Schlieren images of cases 10s – 16s. It can be observed once again that the secondary structure is almost invisible as a result of fuel injection. This can be attributed once more to the fact that newly formed compression fan is taken over by nozzle-rim expansion fan.

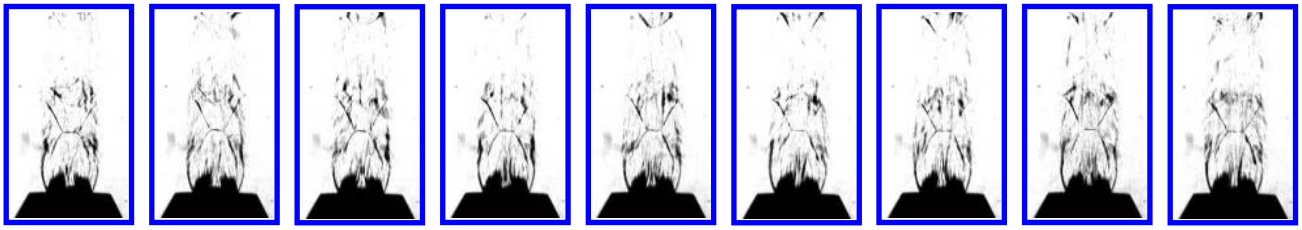

| Case # | 1s | 2s | 3s | 4s | 5s | 6s | 7s | 8s | 9s |
|---|---|---|---|---|---|---|---|---|---|
| $M_{conv}$ = | 1.91 | 1.86 | 1.81 | 1.77 | 1.72 | 1.67 | 1.63 | 1.58 | 1.53 |

**Figure 14. Effect of convective Mach number under swirling no-recess conditions (constant density ratio = 36.73)**

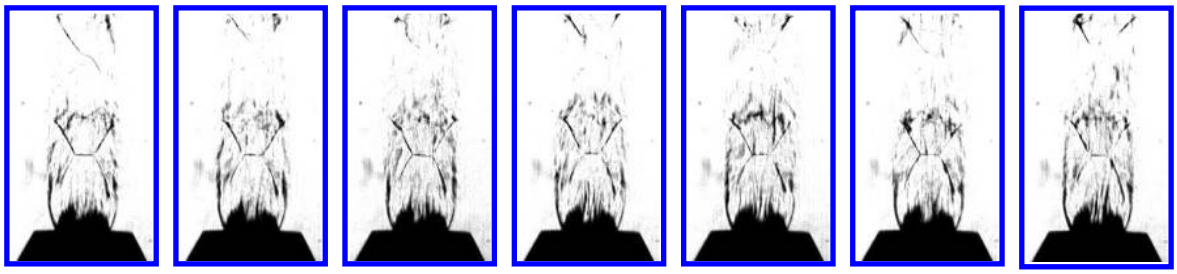

| Case # | 10s | 11s | 12s | 13s | 14s | 15s | 16s |
|---|---|---|---|---|---|---|---|
| DR = | 4.48 | 5.03 | 5.74 | 6.68 | 7.98 | 9.93 | 13.12 |

**Figure 15. Effect of density ratio (DR) under swirling no-recess conditions (constant convective Mach number = 1.42)**



With the secondary structure absent, no significant differences can be observed from one case to another, as the air-fuel density ratio is changed. The single minor difference to be recognized is that the dark region, characteristic of nozzle-rim expansion fan appears to extend to the centerline, as the density ratio is *decreased*. This trend should not be mistaken for an increase in size of expansion fan. Lower density ratios mean higher fuel-jet densities, since air density is constant. The higher the fuel-jet density is, the darker it appears on Schlieren image.

## IV. Conclusions

The effects of convective Mach number, air-fuel density ratio, and imparting swirl to airflow have been investigated experimentally in free under-expanded supersonic-nozzle flow comprising diamond shock structure with coaxial fuel injection. The following conclusions were made: (a) Two distinct diamond shock sub-structures are identifiable, a primary one off nozzle-rim and a secondary structure that is generated due to the existence of coaxial injection system. Both structures are not fully independent of each other. The presence of each partially affects the other. (b) The primary shock sub-structure is affected mainly by properties of airflow. Keeping these unchanged results in an almost constant primary structure that undergoes only minor changes due to its partial dependence on secondary one. (c) The secondary structure, generated off injection system and air-fuel shear layer, is strongly dependent on properties of injected fuel, primarily convective Mach number. (d) Under non-swirling conditions, changing convective Mach number alters the ability of central fuel jet to influence curvature of shear layer and, consequently, the secondary sub-structure it generates. On the other hand, changing air-fuel density ratio at constant convective Mach number does not yield any significant changes in either sub-structure. (e) The strengths of both primary and secondary structures are reduced significantly, if swirl is imparted to airflow. Moreover, the size of nozzle-rim expansion fan increases, and the shape of inner flow boundaries changes, as the centrifugal force pushes flow outwards. (f) Under swirling conditions, decreasing convective Mach number does not affect primary sub-structure significantly, as expected, but the secondary structure weakens with introduction of fuel injection and gradually diminishes with decrease in convective Mach number. A compression fan, which generates the secondary structure, is taken over by the large nozzle-rim expansion fan, resulting in elimination of secondary structure. Therefore, no significant differences can be observed from one case to another, as the air-fuel density ratio is changed.

## Acknowledgments

This work was supported by the Space Vehicle Technology Institute under grant NCC3-989 jointly funded by NASA and DoD within the NASA Constellation University Institutes Project, with Claudia Meyer as the Project Manager. The DoD work was supported by the USAF. This support is gratefully acknowledged.

Assistance provided by Adam Kareem in data acquisition and analysis is much appreciated.

## References

[1]Gruber, M.R., Nejad, A.S., Chen, T.H., and Dutton, J.C., "Mixing and Penetration Studies of Sonic Jets in a Mach 2 Freestream," Journal of Propulsion and Power, Vol. 11, No. 2, March-April 1995.

[2]Kutschenreuter, P., "Supersonic Flow Combustors," Scramjet Propulsion, edited by Curran, E.T. and Murphy, S.N.B., Progress in Astronautics and Aeronautics Series, Vol. 189, 2000, pp. 513 – 567.

[3]Abdelhafez, A., Gupta, A. K., Balar, R., and Yu, K., "Evaluation of Oblique and Traverse Fuel Injection in a Supersonic Combustor," 43rd AIAA/ASME/SAE/ASEE Joint Propulsion Conference & Exhibit, Cincinnati, OH, July 8-11, 2007, AIAA-2007-5026.

[4]Abdelhafez, A. and Gupta, A. K., "Numerical Investigation of Oblique Fuel Injection in Supersonic Combustors," 46th AIAA Aerospace Sciences Meeting and Exhibit, Reno, NV, Jan. 7-10, 2008, AIAA-2008-0068.

[5]Sung, C. J., Li, J. G., Yu, G., and Law, C. K., "Chemical Kinetics and Self-Ignition in a Model Supersonic Hydrogen–Air Combustor," AIAA Journal, Vol. 37, No. 2, February 1999, pp. 208 – 214.

[6]Conaire, M. O., Curran, H. J., Simmie, J. M., Pitz, W. J., and Westbrook, C. K., "A Comprehensive Modeling Study of Hydrogen Oxidation," International Journal of Chemical Kinetics, Vol. 36, Issue 11, pp. 603 – 622.

[7]Ben-Yakar, A., "Experimental Investigation of Transverse Jets in Supersonic Cross-flows," Ph.D. Dissertation, Dept. of Mechanical Eng., Stanford Univ., Stanford, CA, Dec. 2000.

[8]Huh, H., and Driscoll, J. F., "Measured Effects of Shock Waves on Supersonic Hydrogen-Air Flames," 32nd Joint Propulsion Conference and Exhibit, Lake Buena Vista, FL, July, 1996, AIAA- 96-3035.

[9]Yang, J., Kubota, T., and Zukoski, E. E., "Applications of Shock-Induced Mixing to Supersonic Combustion," AIAA Journal, Vol. 31, No. 5, May 1993, pp. 854 – 862.

[10]Menon, S., "Shock-wave-induced mixing enhancement in scramjet combustors," AIAA 27th Aerospace Sciences Meeting, Reno, NV, Jan 1989, AIAA-89-0104.

[11]Cutler, A. D. and Doerner, S. E., "Effects of Swirl and Skew upon Supersonic Wall Jet in Crossflow," Journal of Propulsion and Power, Vol. 17, No. 6, November–December 2001, pp. 1327-1332.

[12]Yu, Y. K., Chen, R. H., and Chew, L., "Screech Tone Noise and Mode Switching in Supersonic Swirling Jets," AIAA Journal, Vol. 36, No. 11, pp. 1968-1974.

[13]Kraus, D. K. and Cutler, A. D., "Mixing of Swirling Jets in a Supersonic Duct Flow," Journal of Propulsion and Power, Vol. 12, No. 1, January–February 1996, pp. 170-177.

[14]Carpenter, P. W., "A Linearized Theory for Swirling Supersonic Jets and Its Application to Shock-Cell Noise," AIAA Journal, Vol. 23, No. 12, 1985, pp. 1902-1909.

[15]Cutler, A. D., Levey, B. S., and Kraus, D. K., "Near-Field Flow of Supersonic Swirling Jets," AIAA Journal, Vol. 33, No. 5, May 1995, pp. 876-881.

[16]Yamasaki, H., Okuno, Y., Torii, S., Masuda, J., Tsutsumi, M., Oda, N., Uchiyama, K., Kouka, H., Fujimoto, T., Suzuki, H., Suzuki, M., and Ohgaki, K., "Improvement of Disk MHD Generator Performance by Inlet Swirl," 30th Plasmadynamics and Lasers Conference, Norfolk, VA, June 28 – July 1, 1999, AIAA-99-3658.

[17]Dutton, J. C., "Swirling Supersonic Nozzle Flow," Journal of Propulsion and Power, Vol. 3, No. 4, 1987, pp. 342-349.

[18]Kitamura, E., Matsumoto, M., Koike, S., and Masuya, G., "PIV Measurement of Supersonic Swirling Jet," Journal of the Visualization Society of Japan, Vol. 22, No. 1, 2002, pp. 189-192.

[19]Yaguchi, H., Suzuki, K., Takita, K., and Masuya, G., "Mixing Enhancement of Supersonic Jet with Swirl," Nippon Kikai Gakkai Ryutai Kogaku Bumon Koenkai Koen Ronbunshu, 2000, pp. 101-104.

[20]Gupta, A. K., Lilley, D. G., and Syred, N., "Swirl Flows," Abacus Press, UK, 1984, ISBN 0-85626-175-0.

[21]Claypole, T. C. and Syred, N., "The Effects of Swirl Burner Aerodynamics on NOx Formation," Proceedings of the Eighteenth Symposium (International) on Combustion, Combustion Inst., Pittsburgh, PA, 1981, pp. 81-89.

[22]Naughton, J. W., Cattafesta, L. N., III, and Settles, G. S., "An Experimental Study of Compressible Turbulent Mixing Enhancement in Swirling Jets," Journal of Fluid Mechanics, Vol. 330, 1997, pp. 271-305.

[23]Panda, J. and McLaughlin, D. K., "Experiments on the Instabilities of a Swirling Jet," Physics of Fluids, Vol. 6, No. 1, 1994, pp. 263-276.